

SEARCH FOR SOLAR AXIONS: THE CAST EXPERIMENT AT CERN

BERTA BELTRÁN⁶
for the CAST collaboration

S. ANDRIAMONJE², V. ARSOV¹³, S. AUNE², D. AUTIERO¹⁷, F. AVIGNONE³, K. BARTH¹,
A. BELOV¹¹, B. BELTRÁN⁶, H. BRÄUNINGER⁵, J. M. CARMONA⁶, S. CEBRIÁN⁶, E. CHESI¹,
J. I. COLLAR⁷, R. CRESWICK³, T. DAFNI⁴, M. DAVENPORT¹, L. DI LELLA¹⁶,
C. ELEFThERiADiS⁵, J. ENGLHAUSER⁵, G. FANOuRAkiS⁹, H. FARACH³, E. FERRER²,
H. FiSCHER¹⁰, J. FRANZ¹⁰, P. FRIEDRICH⁵, T. GERALIS⁹, I. GIOMATARIS², S. GNINENKO¹¹,
N. GOLOUBEV¹¹, R. HARTMANN⁵, M. D. HASINOFF¹², F. H. HEINSIUS¹⁰,
D. H. H. HOFFMANN⁴, I. G. IRASTORZA², J. JACOBY¹³, D. KANG¹⁰, K. KÖNiGSMANN¹⁰,
R. KOTTHAUSt¹⁴, M. KRČMAR¹⁵, K. KOUStOURiS⁹, M. KUSTER^{5,19}, B. LAKIĆ¹⁵, C. LASSEUR¹,
A. LIOLIOS⁸, A. LJUBIĆIĆ¹⁵, G. LUTZ¹⁴, G. LUZÓN⁶, D. W. MILLER⁷, A. MORALES^{6, a},
J. MORALES⁶, M. MUTTERER⁴, A. NIKOLAIDIS⁸, A. ORTiZ⁶, T. PAPAEvANGELOU¹,
A. PLACCI¹, G. RAFFELT¹⁴, J. RUZ⁶, H. RIEGE⁴, M. L. SARSA⁶, I. SAVVIDIS⁸, W. SERBER¹⁴,
P. SERPICO¹⁴, Y. SEMERTZIDIS¹⁸, L. STEWART¹, J. D. VIEIRA⁷, J. VILLAR⁶, L. WALCKIERS¹,
K. ZACHARIADOU⁹ and K. ZIOUTAS⁸
(CAST COLLABORATION)

¹European Organization for Nuclear Research (CERN), Genève, Switzerland

²DAPNIA, Centre d'Études Nucléaires de Saclay (CEA-Saclay), Gif-sur-Yvette, France

³Department of Physics and Astronomy, University of South Carolina, Columbia, SC, USA

⁴GSI-Darmstadt and Institut für Kernphysik, TU Darmstadt, Darmstadt, Germany

⁵Max-Planck-Institut für Extraterrestrische Physik, Garching, Germany

⁶Instituto de Física Nuclear y Altas Energías, Universidad de Zaragoza, Zaragoza, Spain

⁷Enrico Fermi Institute and KICP, University of Chicago, Chicago, IL, USA

⁸Aristotle University of Thessaloniki, Thessaloniki, Greece

⁹National Center for Scientific Research "Demokritos", Athens, Greece

¹⁰Albert-Ludwigs-Universität Freiburg, Freiburg, Germany

¹¹Institute for Nuclear Research (INR), Russian Academy of Sciences, Moscow, Russia

¹²Department of Physics and Astronomy, University of British Columbia, Vancouver, Canada

¹³Johann Wolfgang Goethe-Universität, Institut für Angewandte Physik, Frankfurt am Main, Germany

¹⁴Max-Planck-Institut für Physik (Werner-Heisenberg-Institut), München, Germany

¹⁵Rudjer Bošković Institute, Zagreb, Croatia

¹⁶Scuola Normale Superiore, Pisa, Italy.

¹⁷Inst. de Physique Nucléaire, Lyon, France.

¹⁸Brookhaven Nat. Lab., NY-USA.

¹⁹Technische Universität Darmstadt, IKP, Darmstadt, Germany

Hypothetical axion-like particles with a two-photon interaction would be produced in the sun by the Primakoff process. In a laboratory magnetic field they would be transformed into X-rays with energies of a few keV. The CAST experiment at CERN is using a decommissioned LHC magnet as an axion helioscope in order to search for these axion-like particles. The analysis of the 2003 data¹ has shown no signal above the background, thus implying an upper limit to the axion-photon coupling of $g_{a\gamma} < 1.16 \times 10^{-10} \text{ GeV}^{-1}$ at 95% CL for $m_a \lesssim 0.02 \text{ eV}$. The stable operation of the experiment during 2004 data taking allow us to anticipate that this value will be improved. At the end of 2005 we expect to start with the so-called second phase of CAST, when the magnet pipes will be filled with a buffer gas so that the axion-photon coherence will be extended. In this way we will be able to search for axions with masses up to 1 eV.

1 Introduction

QCD is the universally accepted theory for describing the strong interactions, but it has one serious blemish: the so-called “strong CP problem”. In the following we will give a brief review of it, a more general introduction on the subject can be found in^{2,3}.

Because of the existence of non-trivial vacuum gauge configurations, QCD has a very rich vacuum structure. All these degenerate vacuum configurations of the theory are characterized by the topological winding number n associated with them

$$n = \frac{ig^3}{24\pi^2} \int d^3x \text{Tr} \varepsilon_{ijk} A^i(x) A^j(x) A^k(x) \quad (1)$$

where g is the gauge coupling, A^i is the gauge field, and the temporal gauge ($A^0 = 0$) has been used. Then, the correct vacuum state of the theory is a superposition of all these degenerate states $|n\rangle$,

$$|\Theta\rangle = \sum_n \exp(-in\Theta) |n\rangle \quad (2)$$

where, a priori, the angle Θ is an arbitrary parameter of the theory. States of different Θ are the physically distinct vacua for the theory, each with a distinct world of physics built upon it. By appropriate means the effects of this Θ -vacuum can be recast into a single, additional non-perturbative term in the QCD Lagrangian:

$$\mathcal{L}_{QCD} = \mathcal{L}_{pert} + \bar{\Theta} \frac{g^2}{32\pi^2} G^{a\mu\nu} \tilde{G}_{a\mu\nu}, \quad \bar{\Theta} = \Theta + \text{Argdet} \mathcal{M} \quad (3)$$

where $G^{a\mu\nu}$ is the field strength tensor, $\tilde{G}_{a\mu\nu}$ is its dual, and \mathcal{M} is the quark mass matrix. This extra term in the QCD Lagrangian arises due to two separate and independent effects: the Θ structure of the pure QCD vacuum, and electroweak effects involving the quark masses.

However, such a term in the QCD Lagrangian clearly violates CP, T and P in the case of $\bar{\Theta} \neq 0$, yet Nature has never exhibited this in any experiment. Moreover, the value of the neutron electric dipole moment depends on $\bar{\Theta}$, and the present experimental bound⁴ $d_N < 6.3 \times 10^{-26} \text{ e.cm}$ constrains $\bar{\Theta}$ to be less than (or of the order of) 10^{-10} . The mystery of why the *arbitrary* parameter $\bar{\Theta}$ must be so small is the strong CP problem.

Various theoretical attempts to solve this strong CP problem have been postulated^{2,5}, being the most elegant solution the one proposed by Peccei and Quinn in 1977^{6,7}. Their idea was to make $\bar{\Theta}$ a dynamical variable with a classical potential that is minimized by $\bar{\Theta} = 0$. This is accomplished by introducing an additional global, chiral symmetry, known as PQ (Peccei-Quinn) symmetry $U(1)_{PQ}$, which is spontaneously broken at a scale f_{PQ} . Immediately and independently, Weinberg⁸ and Wilczek⁹ realized that, because $U(1)_{PQ}$ is spontaneously broken, there should be a pseudo-Goldstone boson, “the axion” (or as Weinberg originally referred to it, “the higglet”). Because $U(1)_{PQ}$ suffers from a chiral anomaly, the axion acquires a small mass of the order of $m_a \approx 6 \mu\text{eV} (10^{12} \text{ GeV}/f_{PQ})$.

A priori the mass of the axion (or equivalently the f_{PQ} scale) is arbitrary, but it can be constrained using the data from various experiments, astrophysical considerations (cooling rates of stars) and cosmological arguments (overclosure of the Universe)^{10,11}. Nowadays it is believed to fall inside the so-called “axion mass window”: $10^{-6} \text{ eV} < m_a < 10^{-3} \text{ eV}$. The upper limit depends on the axion-nucleon interaction that it is constrained in two different ways by the observed neutrino signal of supernova (SN)1987A^{12,13}. However, these values rely on the model-dependent axion-nucleon coupling, they involve large statistical and systematical uncertainties, and perhaps unrecognized loop-holes. Therefore, it is prudent to consider other experimental or astrophysical methods to constraint axions in this range of parameters.

The interaction strength of axions with ordinary matter (photons, electrons and hadrons) scales³ as $1/f_{PQ}$ and so the larger this number, the more weakly the axion couples. The present constraints on its mass make the axion a weakly interacting particle, therefore a nice candidate for the Dark Matter of the Universe¹¹.

One generic property of the axions is a two-photon interaction of the form:

$$\mathcal{L}_{a\gamma} = -\frac{1}{4}g_{a\gamma}F_{\nu\mu}\tilde{F}^{\nu\mu}a = g_{a\gamma}\mathbf{E} \cdot \mathbf{B} a \quad (4)$$

where F is the electromagnetic field-strength tensor, \tilde{F} is its dual, and \mathbf{E} and \mathbf{B} the electric and magnetic fields. As a consequence axions can transform into photons in external electric or magnetic fields¹⁴, an effect that may lead to measurable consequences in laboratory or astrophysical observations. For example, stars could produce these particles by transforming thermal photons in the fluctuating electromagnetic field of the stellar plasma^{15,10}, or axions could contribute to the magnetically induced vacuum birefringence, interfering with the corresponding QED effect^{16,17}. The PVLAS¹⁸ experiment apparently observes this effect, although an interpretation in terms of axion-like particles requires a coupling strength far larger than existing limits.

The sun would be a strong axion source and thus offers a unique opportunity to actually detect such particles by taking advantage of their back-conversion into X-rays in laboratory magnetic fields¹⁹. The expected solar axion flux at the Earth due to the Primakoff process is: $\Phi_a = g_{10}^2 3.67 \times 10^{11} \text{ cm}^{-2} \text{ s}^{-1}$ with $g_{10} \equiv g_{a\gamma} 10^{10} \text{ GeV}$, with an approximately thermal spectral distribution given by (Fig. 1):

$$\frac{d\Phi_a}{dE_a} = g_{10}^2 3.821 \times 10^{10} \frac{(E_a/\text{keV})^3}{(e^{E_a/1.103 \text{ keV}} - 1)} \text{ cm}^{-2} \text{ s}^{-1} \text{ keV}^{-1} \quad (5)$$

and an average energy of 4.2 keV^a . The possible flux variations due to solar-model uncertainties are negligible. Axion interactions other than the two-photon vertex would provide for additional production channels, but in the most interesting scenarios these channels are severely constrained, leaving the Primakoff effect as the dominant one¹⁰. In any case, it is conservative to use the Primakoff effect alone when deriving limits on $g_{a\gamma}$.

2 Principle of detection

A particularly intriguing application of magnetically induced axion-photon conversions is to search for solar axions using an “axion helioscope” as proposed by Sikivie¹⁹. One looks at the sun through a “magnetic telescope” and places an X-ray detector at the far end. Inside the magnetic field, the axion couples to a virtual photon, producing a real photon via the Primakoff effect: $a + \gamma_{\text{virtual}} \Rightarrow \gamma$. The energy of this photon is then equal to the axion’s total energy.

^aThe spectrum in²⁰ has been changed to that proposed in²¹, however with a modified normalization constant to match the total axion flux used here, which is predicted by a more recent solar model

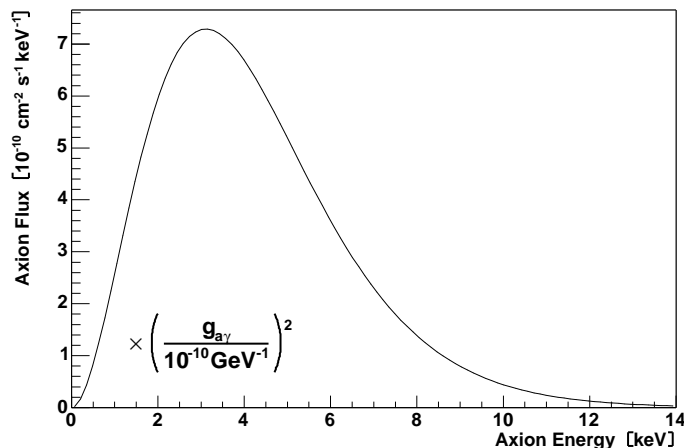


Figure 1: Axion flux spectrum at the Earth

The expected number of these photons that reach the X-ray detector is:

$$N_\gamma = \int \frac{d\Phi_a}{dE_a} P_{a \rightarrow \gamma} S T dE_a \quad (6)$$

where $d\Phi_a/dE_a$ is the axion flux at the Earth as given by eq.(5), S is the magnet bore area (cm^2), T is the measurement time (s) and $P_{a \rightarrow \gamma}$ is the conversion probability of an axion into a photon. If we take some realistic numbers ($g_{a\gamma} = 10^{-10} \text{ GeV}^{-1}$, $T = 100 \text{ h}$ and $S = 15 \text{ cm}^2$) this number of photons would be nearly 30 events.

The conversion probability in vacuum is given by:

$$P_{a \rightarrow \gamma} = \left(\frac{B g_{a\gamma}}{2} \right)^2 2L^2 \frac{1 - \cos(qL)}{(qL)^2} \quad (7)$$

where B and L are the magnetic field and its length (given in natural units), and $q = m_a^2/2E$ is the longitudinal momentum difference between the axion and an X-ray of energy E . The conversion process is coherent when the axion and the photon fields remain in phase over the length of the magnetic field region. The coherence condition states that^{23,24} $qL = < \pi$ so that a coherence length of 10 m in vacuum requires $m_a \lesssim 0.02 \text{ eV}$ for a photon energy 4.2 keV. Coherence can be restored for a solar axion rest mass up to $\sim 1 \text{ eV}$ by filling the magnetic conversion region with a buffer gas²⁰ so that the photons inside the magnet pipe acquire an effective mass whose wavelength can match that of the axion. For an appropriate gas pressure, coherence will be preserved for a narrow axion mass window. Thus, with the proper pressure settings it is possible to scan for higher axion masses.

The first implementation of the axion helioscope concept was performed at BNL²³. More recently, the Tokyo axion helioscope²⁵ with $L = 2.3 \text{ m}$ and $B = 3.9 \text{ T}$ has provided the limit $g_{10} < 6.0$ at 95% CL for $m_a \lesssim 0.03 \text{ eV}$ (vacuum) and $g_{10} < 6.8\text{--}10.9$ for $m_a \lesssim 0.3 \text{ eV}$ (using a variable-pressure buffer gas)²⁶. Limits from crystal detectors^{27,28,29} are much less restrictive.

3 CAST experiment

In order to detect solar axions or to improve the existing limits on $g_{a\gamma}$ an axion helioscope has been built at CERN by refurbishing a decommissioned LHC test magnet²⁴ which produces a

magnetic field of $B = 9.0$ T in the interior of two parallel pipes of length $L = 9.26$ m and a cross-sectional area $S = 2 \times 14.5$ cm². The aperture of each of the bores fully covers the potentially axion-emitting solar core ($\sim 1/10$ th of the solar radius). The magnet is mounted on a platform with $\pm 8^\circ$ vertical movement, allowing for observation of the sun for 1.5 h at both sunrise and sunset. The horizontal range of $\pm 40^\circ$ encompasses nearly the full azimuthal movement of the sun throughout the year. The time the sun is not reachable is devoted to background measurements. A full cryogenic station is used to cool the superconducting magnet down to 1.8 K needed for its superconducting operation³⁰. The hardware and software of the tracking system have been precisely calibrated, by means of geometric survey measurements, in order to orient the magnet to any given celestial coordinates. The overall CAST pointing precision is better³¹ than 0.01° including all sources of inaccuracy such as astronomical calculations, as well as spatial position measurements. At both ends of the magnet, three different detectors have searched for excess X-rays from axion conversion in the magnet when it was pointing to the sun. Covering both bores of one of the magnet’s ends, a conventional Time Projection Chamber (TPC) is looking for X-rays from “sunset” axions. At the other end, facing “sunrise” axions, a second smaller gaseous chamber with novel MICROMEGAS (micromesh gaseous structure – MM)³² readout is placed behind one of the magnet bores, while in the other one, a X-ray mirror telescope is used with a Charge Coupled Device³³ (pn-CCD) as the focal plane detector. Both the pn-CCD and the X-ray telescope are prototypes developed for X-ray astronomy³⁴. The X-ray mirror telescope can produce an “axion image” of the sun by focusing the photons from axion conversion to a ~ 6 mm² spot on the pn-CCD. The enhanced signal-to-background ratio substantially improves the sensitivity of the experiment.

3.1 First phase of CAST

During the years 2003 and 2004 the CAST experiment has gone through the so-called first phase, where the data has been taken with vacuum inside the magnetic field area, so that we were sensitive to axion masses up to $m_a \lesssim 0.02$ eV as explained in section 2.

3.2 Second phase of CAST

In order to extend the range of axion masses to which we are sensitive, the magnet pipes will be filled with Helium gas in phase II. As explained in section 2, a gas with a given pressure will provide a refractive photon mass so that the coherence of the photon and axion fields will be restored for a certain range of axion masses. The second phase of the experiment is very challenging because, for the first time, a laboratory experiment will search for axions in the theoretically motivated range of axion parameters (see Fig. 2).

Data taking for this second phase it is scheduled to begin at the end of 2005, with low pressure ⁴He gas inside the pipes at 1.8 K, the magnet’s operating temperature. There is a limit in the pressure that we can reach with ⁴He before it liquefies, so in order to be able to extend the mass axion searches up to ~ 0.82 eV we will have to switch to ³He, which has a higher vapor pressure. These steps are scheduled to occur during 2006 and 2007.

Beyond these plans CAST could search for axions with still higher masses up to ~ 1.4 eV with the actual set-up, by installing thermally isolated gas cells inside the magnet bores. This would allow us to work at higher temperatures (~ 5.4 K) so that we could reach higher pressures and densities of the ⁴He buffer gas.

4 Data analysis and first results

4.1 2003 data taking

CAST operated for about 6 months from May to November in 2003, during most of which time at least one detector was taking data. The results¹ presented in this paper were obtained after the analysis of the data sets listed in Table 1. An independent analysis was performed for each data set. Finally, the results from all data sets are combined.

An important feature of the CAST data treatment is that the detector backgrounds are measured with ~ 10 times longer exposure during the non-alignment periods. The use of these data to estimate and subtract the true experimental background during sun tracking data is the most sensitive step in the CAST analysis. To assure the absence of systematic effects, the main strategy of CAST is the use of three independent detectors with complementary approaches. In the event of a positive signal, it should appear consistently in each of the three detectors when it is pointing at the sun. In addition, an exhaustive recording of experimental parameters was done, and a search for possible background dependencies on these parameters was performed. A dependence of the TPC background on the magnet position was found, caused by its relatively large spatial movements at the far end of the magnet, which resulted in appreciably different environmental radioactivity levels. Within statistics, no such effect was observed for the sunrise detectors which undergo a much more restricted movement. To correct for this systematic effect in the TPC data analysis, an effective background spectrum is constructed only from the background data taken in magnet positions where sun tracking has been performed and this is weighted accordingly with the relative exposure of the tracking data. Further checks have been performed in order to exclude any possible systematic effect. They were based on rebinning the data, varying the fitting window, splitting the data into subsets and verifying the null hypothesis test in energy windows or areas of the detectors where no signal is expected. In general, the systematic uncertainties are estimated to have an effect of less than $\sim 10\%$ of the final upper limits obtained.

For a fixed m_a , the theoretically expected spectrum of axion-induced photons has been calculated and multiplied by the detector efficiency curves of the detectors, including all hardware and software efficiency losses, such as window transmissions (for TPC and MM), X-ray mirror reflectivity (for pn-CCD), detection efficiency and dead time effects. These spectra, which are proportional to $g_{a\gamma}^4$, are directly used as fit functions to the experimental subtracted spectra (tracking minus background) for the TPC and MM. For these data, the fitting is performed by standard χ^2 minimization. Regarding the pn-CCD data, the analysis is restricted to the small area on the pn-CCD where the axion signal is expected after the focusing of the X-ray telescope. During the data taking period of 2003 a continuous monitoring of the pointing stability of the X-ray telescope was not yet possible, therefore a signal area larger than the size of the sun spot had to be considered. Taking into account all uncertainties of the telescope alignment, the size of the area containing the signal was conservatively estimated to be 34×71 pixels (54.3 mm^2). As in the other detectors, the background is defined by the data taken from the same area

Table 1: Data sets included in our result.

Data set	Tracking exposure(h)	Background exposure(h)	$(g_{a\gamma}^4)_{\text{bestfit}} (\pm 1\sigma \text{ error})$ ($10^{-40} \text{ GeV}^{-4}$)	$\chi_{\text{null}}^2/\text{d.o.f}$	$\chi_{\text{min}}^2/\text{d.o.f}$	$g_{a\gamma}(95\%)$ ($10^{-10} \text{ GeV}^{-1}$)
TPC	62.7	719.9	-1.1 ± 3.3	18.2/18	18.1/17	1.55
MM set A	43.8	431.4	-1.4 ± 4.5	12.5/14	12.4/13	1.67
MM set B	11.5	121.0	2.5 ± 8.8	6.2/14	6.1/13	2.09
MM set C	21.8	251.0	-9.4 ± 6.5	12.8/14	10.7/13	1.67
pn-CCD	121.3	1233.5	0.4 ± 1.0	28.6/20	28.5/19	1.23

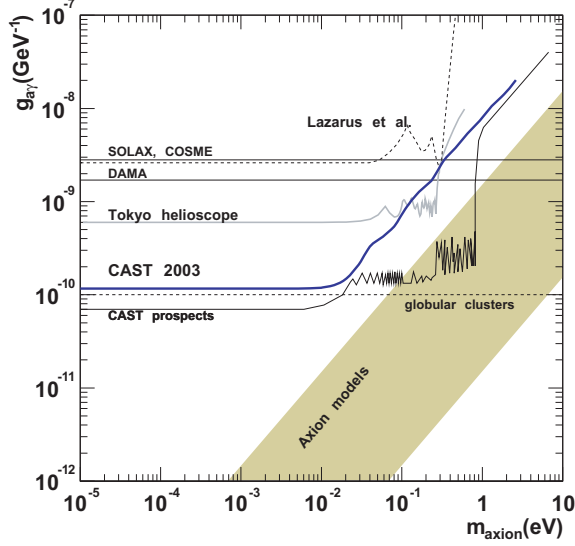


Figure 2: Exclusion limit (95% CL) from the CAST 2003 data compared with other constraints discussed in section 2. The shaded band represents typical theoretical models. Also shown is the future CAST sensitivity as foreseen in the experiment proposal.

during the non-tracking periods, but, in addition, the background in the signal area was also determined by extrapolating the background measured during tracking periods in the part of the pn-CCD not containing the sun spot. Both methods of background selection led to the same final upper limit on the coupling constant $g_{a\gamma}$. The resulting low counting statistics in the pn-CCD required the use of a likelihood function in the minimization procedure, rather than a χ^2 -analysis. The best fit values of $g_{a\gamma}^4$ obtained for each of the data sets are shown in Table 1, together with their 1σ error and the corresponding χ_{\min}^2 values and degrees of freedom. Each of the data sets is individually compatible with the absence of any signal as can be seen from the χ_{null}^2 values shown in Table 1. The excluded value of $g_{a\gamma}^4$ was conservatively calculated by taking the limit encompassing 95% of the physically allowed part (i.e. positive signals) of the Bayesian probability distribution with a flat prior in $g_{a\gamma}^4$. The described procedures were done using $g_{a\gamma}^4$ instead of $g_{a\gamma}$ as the minimization and integration parameter because the signal strength (i.e. number of counts) is proportional to $g_{a\gamma}^4$. The 95% CL limits on $g_{a\gamma}$ for each of the data sets are shown in the last column of Table 1. They can be statistically combined by multiplying the Bayesian probability functions and repeating the previous process to find the combined result for the 2003 CAST data:

$$g_{a\gamma} < 1.16 \times 10^{-10} \text{GeV}^{-1} (95\% \text{CL}). \quad (8)$$

Thus far, our analysis was limited to the mass range $m_a \lesssim 0.02$ eV where the expected signal is mass-independent because the axion-photon oscillation length far exceeds the length of the magnet. For higher m_a the overall signal strength diminishes rapidly and the spectral shape differs. Our procedure was repeated for different values of m_a to obtain the entire 95% CL exclusion line shown in Fig. 2.

4.2 2004 data taking

The data taken from 2004 have not yet been fully analyzed. However, the stable operation of the experiment allowed the CAST collaboration to take enough high-quality data to anticipate that the final sensitivity will be close to the value presented in the CAST proposal (see Fig. 2)

5 Summary

The origin of the axion as a particle that solves the strong CP problem has been reviewed. Some properties of this pseudo-scalar particle have been pointed out, among them the fact that it can transform into a photon in external electric or magnetic fields, this being the only property of the axion on which CAST relies. The CAST experiment and its first results¹ have been presented. Our limit improves the best previous laboratory constraints²⁵ on $g_{a\gamma}$ by a factor 5 in our coherence region $m_a \lesssim 0.02$ eV. A higher sensitivity is expected from the 2004 data with improved conditions in all detectors, which should allow us to surpass the astrophysical limit. In addition, starting in 2005, CAST plans to take data with a varying-pressure buffer gas in the magnet pipes, in order to restore coherence for axion masses above 0.02 eV. The extended sensitivity to higher axion masses will allow us to enter into the region shown in Fig. 2 which is especially motivated by axion models³⁵.

References

1. K. Zioutas *et al.* [CAST Collaboration], Phys. Rev. Lett. **94** (2005) 121301
2. C. Jarlskog(Ed), “*CP violation*” World Scientific (1989)
3. M. S. Turner, “Windows On The Axion,” Phys. Rep. **197**, 67 (1990).
4. P. G. Harris *et al.*, Phys. Rev. Lett. **82** (1999) 904.
5. M. Dine, [arXiv:hep-ph/0011376].
6. R. D. Peccei and H. R. Quinn, Phys. Rev. D **16** (1977) 1791.
7. R. D. Peccei and H. R. Quinn, Phys. Rev. Lett. **38** (1977) 1440.
8. S. Weinberg, Phys. Rev. Lett. **40**, 223 (1978).
9. F. Wilczek, Phys. Rev. Lett. **40**, 279 (1978).
10. G. G. Raffelt, Ann. Rev. Nucl. Part. Sci. **49**, 163 (1999) [arXiv:hep-ph/9903472].
11. S. Eidelman *et al.* [Particle Data Group], Phys. Lett. B **592** (2004) 1.
12. J. R. Ellis and K. A. Olive, Phys. Lett. B **193** (1987) 525.
13. G. Raffelt and D. Seckel, Phys. Rev. Lett. **60** (1988) 1793.
14. H. Primakoff, Phys. Rev. **81**, 899 (1951).
15. D. A. Dicus, E. W. Kolb, V. L. Teplitz and R. V. Wagoner, Phys. Rev. D **18** (1978) 1829.
16. L. Maiani, R. Petronzio and E. Zavattini, Phys. Lett. B **175** (1986) 359.
17. G. Raffelt and L. Stodolsky, Phys. Rev. D **37** (1988) 1237.
18. G. Cantatore *et al.*, in Proceedings of the 5th International Workshop on the Identification of Dark Matter, Edinburgh, UK, 2004 (to be published). Also see U.Gastaldi in this volume.
19. P. Sikivie, Phys. Rev. Lett. **51**, 1415 (1983) [Erratum-ibid. **52**, 695 (1984)].
20. K. van Bibber *et al.*, Phys. Rev. D **39**, 2089 (1989).
21. R. J. Creswick *et al.*, Phys. Lett. B **427**, 235 (1998).
22. J. N. Bahcall, M. H. Pinsonneault and S. Basu, Astrophys. J. **555**, 990 (2001).
23. D. M. Lazarus *et al.*, Phys. Rev. Lett. **69**, 2333 (1992).
24. K. Zioutas *et al.*, Nucl. Instrum. Meth. A **425** (1999) 480 [arXiv:astro-ph/9801176].
25. S. Moriyama *et al.*, Phys. Lett. B **434**, 147 (1998).
26. Y. Inoue *et al.*, Phys. Lett. B **536**, 18 (2002).
27. F. T. Avignone *et al.*, Phys. Rev. Lett. **81**, 5068 (1998).
28. A. Morales *et al.*, Astropart. Phys. **16**, 325 (2002).
29. R. Bernabei *et al.*, Phys. Lett. B **515** 6 (2001).
30. K. Barth *et al.*, Proc. 2003 Cryogenic Engineering Conference (CEC) and Cryogenic Materials Conference (ICMC).
31. http://cast.web.cern.ch/CAST/edited_tracking.mov
32. Y. Giomataris *et al.*, Nucl. Instrum. Meth. A **376** 29 (1996).

33. L. Struder *et al.*, *Astron. Astrophys.* **365**, L18 (2001).
34. J. Altmann *et al.*, in *Proceedings of SPIE: X-Ray Optics, Instruments, and Mission*, 1998, edited by Richard B. Hoover and Arthur B. Walker, p. 350; J. W. Egle *et al.*, *ibid.*, p. 359; P. Friedrich *et al.*, *ibid.*, p. 369.
35. D. B. Kaplan, *Nucl. Phys. B* **260**, 215 (1985).